The link between a negative high resolution resist contrast/developer performance and the Flory-Huggins parameter estimated from the Hansen solubility sphere.

Deirdre L. Olynick[a], Weilun L. Chao[b], Mark D. Lewis[a], Haoren Lu[c], Scott D. Dhuey[a], and J. Alexander Liddle[d]*

[a]Molecular Foundry and [b]Center for X-ray Optics, Lawrence Berkeley National Laboratory, Berkeley, 1 Cyclotron Road, Berkeley, CA 94720

*DLOlynick@lbl.gov

[c]Now at Nextant, Inc. San Francisco, CA

[d]Now at National Institute of Standards, Gaithersburg, MD

Abstract

We have implemented a technique to identify candidate polymer solvents for spinning, developing, and rinsing for a high resolution, negative electron beam resist hexa-methyl acetoxy calix(6)arene to elicit the optimum pattern development performance. Using the

three dimensional Hansen solubility parameters for over 40 solvents, we have constructed a Hansen solubility sphere. From this sphere, we have estimated the Flory Huggins interaction parameter for solvents with hexa-methyl acetoxy calix(6)arene and found a correlation between resist development contrast and the Flory-Huggins parameter. This provides new insights into the development behavior of resist materials which are necessary for obtaining the ultimate lithographic resolution.

Keywords electron beam lithography, calixarene, Flory-Huggins interaction parameter, chi, Hansen solubility sphere, solvent-polymer interactions

Introduction

Understanding polymer-solvent interactions is key for numerous nanoscience applications. For instance choice of casting solvent can affect morphological evolution of solar-cell polymers.[1] These polymer-solvent issues are particularly relevant in nanolithography where researchers desire small feature patterning of polymer systems in the sub-10 nm regime for applications in areas such as nanoelectronics, nanoelectromechanical and nanobiological systems. Electron beam lithography is a proven technique for creating sub-30 nm patterns with resolution demonstrated down to 6 nm for isolated features in calixarene.[2] In addition, it is effective for templating self-assembly at or below the resolution of the written template, for example, to create patterns of nanocrystals for quantum dots and patterns of block copolymers.[3] To push the resolution further, and to make lithographic polymers compatible with subsequent

processing, understanding the interactions of solvents and the resist during development and other wet processing steps is important.

Fujita, et.al.[4] first demonstrated hexaacetate p-methylcalix[6]arene (henceforth "calixarene" or "MC6AOAc") as a negative e-beam resist and found isolated line resolution of 10 nm, low sidewall roughness, and high etching resistance for a carbon based resist material. This material's main drawback is its low sensitivity (the doses required are ~10-20 times higher than that those for hydrogen silsesquioxane (HSQ) or polymethly methacrylate (PMMA) resists.). However, calixarene still exhibits one of the highest resolutions for a negative electron beam resist material.[2]

There is considerable evidence that lithographic resolution is often limited by development conditions, leading to poor contrast, swelling, line edge roughness, micellization and collapse, and not by the incident electron beam size. For instance, with calixarene resist, Fujita et. al. [5] demonstrated the minimum resolvable feature of 10 nm was independent of e-beam energy (varied from 10 to 50 keV) and found collapse was dose dependent. Yasin, et. al. [2] showed better line acuity is achieved using ultrasonic versus dip development. These authors demonstrated 6 nm isolated lines in calixarene using ultrasonic development and a 2-3 nm probe size. Dense features in this size regime are more difficult to achieve and making optimized development essential.

One limiting factor in the development of resist materials is swelling of the resist. Swelling has been a known problem for decades, particularly for solvent-developed negative resists,[6] and becomes more important as features sizes shrink. It has also been recently identified as an issue for line-edge roughness in aqueous base developed resists[7].

Namaste, et. al. stated[8] swelling can be mitigated by "choosing polymer-solvent combinations with low interaction, that is, a high interaction parameter, χ, [Flory-Huggins interaction parameter, depends on polymer/solvent combination], using a low molecular weight polymer, and adding a network-forming monomer that is polyfunctional and compatible in monomeric and polymeric states with the host polymer" [typical in chemically amplified systems].

In this paper, we have studied the development of a calixarene, a single component cross-linking resist with a low molecular weight material (MC6AOAc, M_w = 972). The low molecular weight mitigates swelling although there is considerable trade-off with regard to sensitivity - nominally 20 mC at 100 kV. To choose the optimum developer solvents, we constructed a three dimensional Hansen solubility sphere for calixarene to find its solubility parameter and use it to estimate χ for solvents interacting with calixarene. We then measured contrast curves for several solvents, and used the estimated χ's to systematically link polymer thermodynamics to contrast behavior and pattern quality. This is a semi-quantitive technique for estimating χ, which requires minimal instrumentation and allows one to choose appropriate solvents for e-beam lithography and wet polymer processing issues in general and understand how χ is linked to contrast and pattern quality.

Background

In earlier work Novembre et. al.[9] used a simplified, two dimensional Hansen solubility map, derived for a resist polymer with several solvents, as an aid in selecting appropriate development and rinse solvents for lithographic processing. The technique is very useful because it only requires a simple binary probe of dissolution with the non irradiated polymer.

In this paper, for a more accurate measurement of the polymer solubility parameter and its interaction with solvents, we use a three dimensional Hansen solubility map and fit the Hansen solubility sphere (Fig. 1). In this way, we have a predictive tool for solvent solubility with the polymer of interest not only with the tested solvents but for any solvents whose solubility parameters are known. Fortunately, Hansen solubility values are tabulated for 100's of solvents.[10]

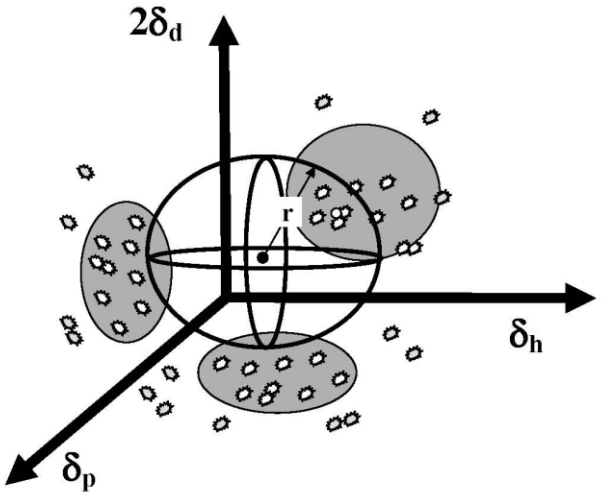

Figure 1. Schematic of the Hansen Solubility sphere. Each axes is one of the three component Hansen solubility parameters, δ_d, δ_h, or δ_p (representing the magnitude of the dispersive or van der waals forces, the hydrogen bonding,

and the polar bonding respectively). The center of the sphere (black dot) represents the three dimensional solubility parameter for the polymer being tested. The sphere with radius "r" encompasses the solubility parameters for all solvents that will solubilize the polymer. The projections of the sphere are shown by the large grey circles (projections are often used to get solubility behavior trends). Tested solvents which will solubilize the polymer will have solubility parameters which lie within the sphere ($\Delta G_{mix}<0$, white markers) and solvents which do not will lie outside the sphere ($\Delta G_{mix}>0$, small grey markers). At the sphere boundary, $\Delta G_{mix} = 0$.

The Hansen solubility parameter is based on the original solubility parameter of Hildebrand and Scott,[11] now called the Hildebrand solubility parameter, has been shown to be effective at describing the behavior of non-polar, non-associating systems. It is defined in terms of the cohesive pressure of the system which can be in turn be related to the cohesive energy density, U, per unit volume, V,

$$\delta = -\left(\frac{U}{V}\right)^{1/2} \quad (1)$$

Hansen[10] extended the Hildebrand parameter by proposing that the cohesive energy density could be broken into several parts to take into account polar and hydrogen bonding:

$$\delta_t^2 = \delta_d^2 + \delta_p^2 + \delta_h^2 \qquad (2)$$

where δ_t is the Hansen solubility parameter (HSP) and δ_d, δ_p, and δ_h represent contributions due to dispersion (van der Waals), polar, and hydrogen-bonding forces respectively. The total HSP should equal the Hildebrand parameter. Since its inception, this parameter has been used extensively to look at interactions between polymers and different solvents, including swelling and solvency behavior. A Hansen solubility sphere (HSP) can be drawn to describe a radius of interaction for a polymer with many different solvents where the plot axes are $2\delta_d$, δ_p, and δ_h (Fig.1). Note that the factor of 2 associated with δ_d is used to generate a sphere rather than an ellipse.[12] The center of the sphere is associated with the polymer solubility parameter. The polymer is soluble in solvents within the sphere boundary where ΔG of mixing is less than zero. The polymer is insoluble in solvents which lie outside the sphere boundary where ΔG of mixing is greater than zero. At the sphere boundary, ΔG of mixing is zero.

If the HSP of the polymer is not known, it can be measured by checking solvency in solvents with known solubility parameters (many 100's are tabulated.[10]) and fitting the data with a sphere where the center is the polymer solubility parameter This is what we have done with our resist, MC6AOAc. This fit is of course temperature dependent with increases in temperature increasing the radius of the sphere and decreases in temperature decreasing the radius.

Novembre, et. al.[9] proposed that solvents which lie just inside the boundary would be optimum for development of a negative resist because the unexposed material would still be soluble, but swelling will be minimized because the polymer/solvent combination would have the least affinity for each other. This can be taken a step further by using the sphere to estimate the Flory-Huggins interaction parameter from the HSP.

Using the geometric mean approximation, the exchange energy density of two components mixing is

$$^{ij}A = (^{i}\delta - ^{j}\delta)^2 \quad (3)$$

where δ is the Hildebrand solubility parameters of components i and j. For the Hansen solubility parameters this becomes[12]

$$^{ij}A = \left[(^{i}\delta_d - ^{j}\delta_d)^2 + .25(^{i}\delta_p - ^{j}\delta_p)^2 + .25(^{i}\delta_h - ^{j}\delta_h)^2\right] \quad (4)$$

where the factor of 0.25, like the plotting of the dispersion interactions on a 2x axis, is to provide a spherical, rather than elliptical representation of the interaction parameter. Here, ^{ij}A has units of MPa.

The Flory-Huggins interaction parameter, χ, can then be found from the exchange energy density as

$$\chi = \frac{V_s\, ^{ij}A}{RT} \quad (5)$$

where V_s is the molar volume of the solvent, R is the molar gas constant and T is the temperature. So, by measuring the Hansen Solubility Parameter for the resist of interest,

we can find ${}^{ji}A$ for each solvent, estimate the χ parameter, and relate it to resist performance.

Experimental

One gram of calixarene (MC6AOAc, TCI America) was dissolved in 20 grams of chlorobenzene and 4 grams of dichloromethane to make a 4% solution. The material was spun coat at 1000 rpm to form a 100 nm film. Films were dipped in room temperature solvents to determine solubility. MC6AOAc was considered soluble if all of it dissolved in less than 15 seconds, slightly soluble if there was some thickness loss after 30 seconds time, and insoluble otherwise. For the samples tested that were classified as insoluble or slightly soluble, the film thickness was measured after 30 seconds and 3 minutes submersion in the solvent using a stylus profilometer (Tencor Alpha-Step 500) scanned over a scratch in the resist. Table 1 shows the list of solvents tested, their solubility parameters, and the room temperature solubility with calixarene. Typically, for solvents that totally solubilized the film, the film was gone in less than 10 seconds.

A sub-set of these solvents were tested as developers for e-beam exposed calixarene. An array of 1 micron squares exposed using a 100 keV electron beam exposure tool (Leica VB6 HR) with a progressive dose were patterned to generate contrast curves. Squares were placed 5 microns apart on a 5 x 5 array. After development, the height of these squares was measured by atomic force microscopy (Digital Instruments Dimension 3100). This AFM was calibrated for the measurement of 70 nm step heights. The scanned image of the array was 40 microns per side. Images were processed using a

flattening and rolling ball scheme and then the heights of each square were measured relative to the background.

Grating patterns were electron beam exposed at a beam current of 520 pA at various doses to look at line pattern resolution and process latitude (exact doses used accompany the images in the text). After exposure, films were dip developed in solvents for 30 seconds, followed by 5 sec dip rinse in isopropyl alcohol. Resists were then blown dry using a dry nitrogen gun. Gratings were then imaged top down at 5 keV using a scanning electron microscope (SEM, Leo 1560).

Results

A. Generation of Hansen Solubility Sphere and χ values for each solvent

Table 1 shows the list of solvents used to test calixarene solubility, their Hansen solubility parameters, and their classification as to how calixarene dissolves in the solvent: soluble (Y), insoluble (N), or slightly soluble. To generate the solubility sphere, the solubility parameters were plotted in three dimensions where the axes are $2\delta_d$, δ_p, and δ_h. A sphere fitting routine was used to find the sphere center and radius of a sphere that encompassed all the solvents and excluded all the non-solvents. Four solvents were classified as slightly soluble; however, only isoamyl alcohol showed a response clearly outside any thickness measurement error (50 nm in 30 seconds). This solvent was set to be near the sphere boundary during the fitting process. The fitting program used is shown in Appendix 1 and based on the program presented by Gharagheizi.[13] The parameters being fit are the center of the sphere, which corresponds to the Hansen

solubility parameter for the solute (here, calixarene) and the radius. Several sphere solutions were found to satisfy the tested solvents. We used several approaches to narrow them down to 15 fits (described in appendix 1) and reached an average center value of δ_d=19.78, δ_p=11.02, and δ_h=4.67 with the average radius being 11.76 with standard deviations for the 15 fits of 0.142, 0.278, 0.500 (δ_d, δ_p, δ_h) and 0.563 (radius) Using equations 3 and 5, and the calixarene Hansen solubility parameter value determined from the fit of the solubility sphere, we estimated χ values each of the solvents tested that solubilize calixarene (Table 2). Each χ value shown is an average value for the 15 sphere fits (each sphere fit will yield a different χ value for each solvent, we averaged the χ's for each solvent from the 15 fits).

Not only does determination of the solubility sphere allow one to rank relevant interactions between the solvents tested and polymer, it is a powerful predictive model; for solvents with a known solubility parameters (close to 1000 are already tabulated.[10, 12]), we can rank the strength of the interaction using the solubility sphere and χ (The uncertainty in the fits of course determine the ability to discern interaction strengths of materials with similar χ . This uncertainty is discussed in appendix 1).

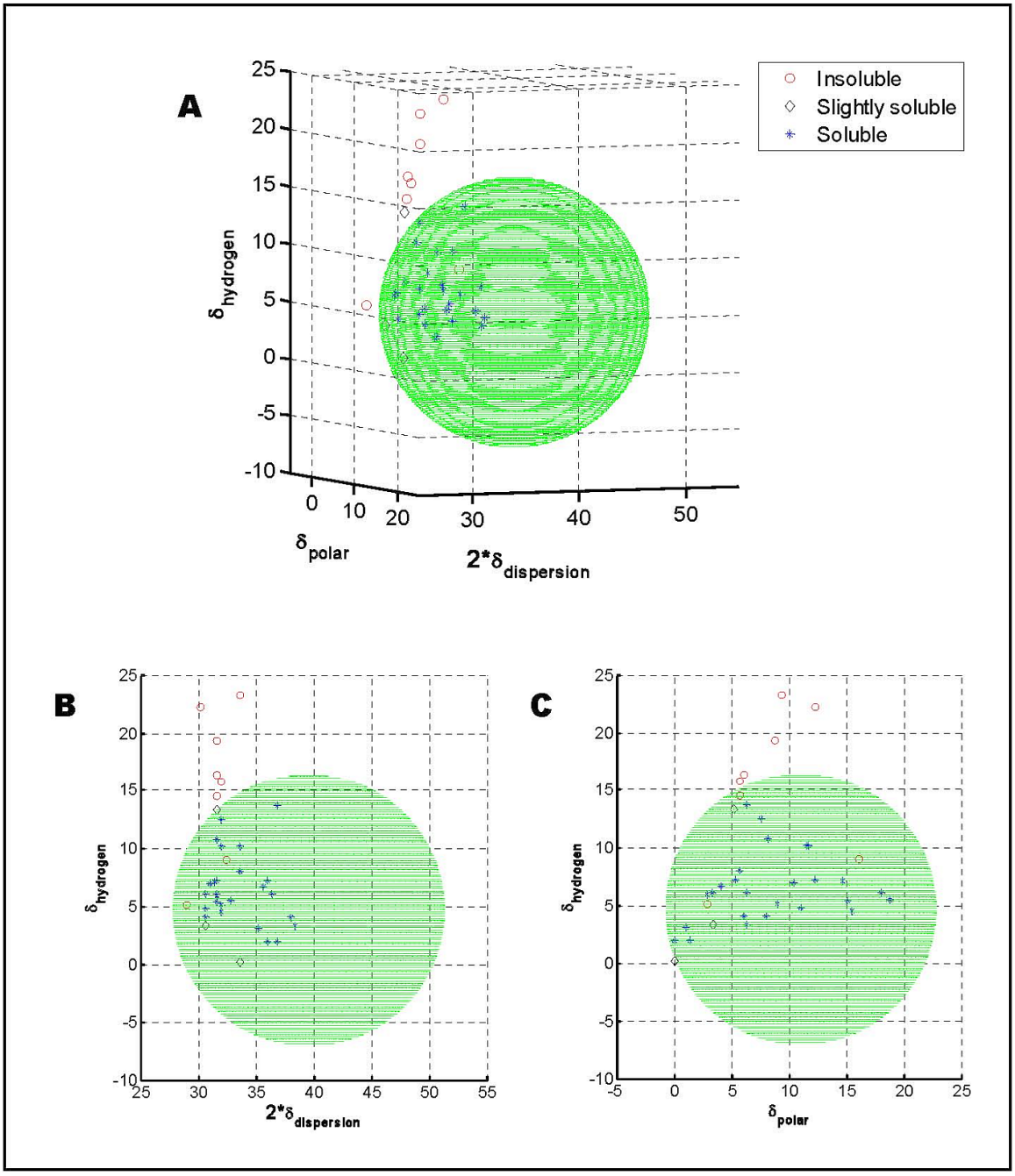

Figure 2. Hansen solubility sphere for calixarene using the average fit values (see text). A) 3 –D representation B) Projection into the hydrogen-dispersion plane C) Projection in the hydrogen-polar plane.

Contrast Curves and SEM images

Contrast curves for development of electron beam exposed calixarene by four solvents, xylenes, toluene, anisole, and NMP, in order from highest to lowest χ values are shown in Figure 3 with SEM images of 20 nm half-pitch developed grating patterns shown in Figure 4. These solvents were chosen because they have χ values that differ beyond experimental errors associated with the Hansen sphere fitting. Lines A and B, Fig. 3, are marked for later discussion. For decreasing χ values (increasing interaction), the contrast and gel dose are higher. This generally indicates better resolution. However, the grating pattern quality decreases with decreasing χ values due to swelling and collapse. Yet, actual resolution of individual lines with the smaller χ values is better as predicted by the contrast curve. The role swelling plays in the contrast and pattern quality is important to understanding the contrast, process latitude, and resolution and is discussed in the subsequent section.

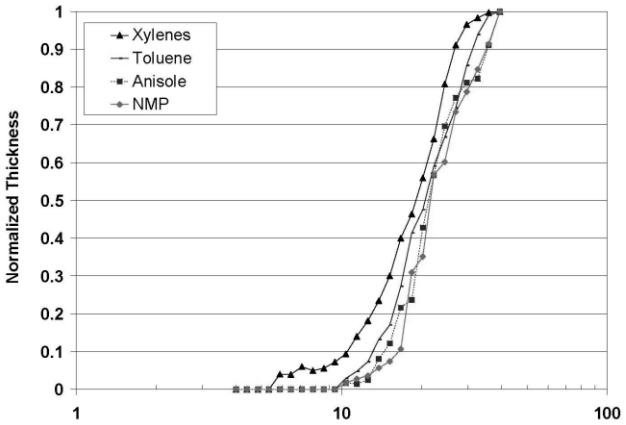

Figure 3. Contrast curves for four solvent developers of calixarene. The χ values are xylenes = 1.52, toluene = 1.21, anisole = 0.81, and NMP =

0.20. As the χ value decreases, the gel dose and contrast increase.

Discussion

Thermodynamics of swelling

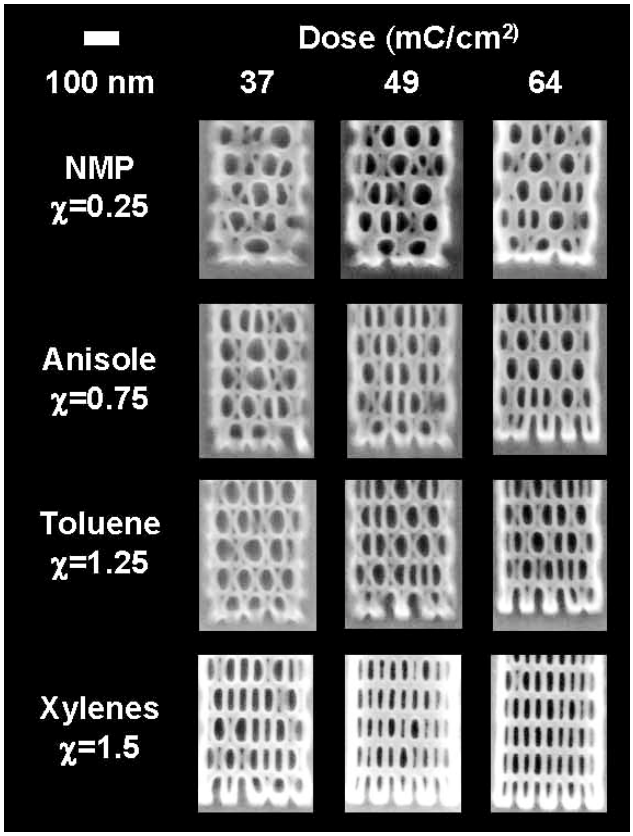

Figure 4. SEM images of the four solvent developers of calixarene whose contrast curves are shown in Fig. 3. Even though the lower χ values (i.e. anisole and NMP) can give better individual line resolution, the overall grating quality decreases due to swelling and pattern collapse.

Having the estimated χ values found from the measured and fit Hansen sphere, we can now apply the Flory-Rehner model for the swelling of networks.[14, 15] The Flory-Rehner model assumes a linear superposition of the mixing and elastic free energies due to swelling of the network. For a lightly cross-linked system undergoing swelling, we can solve for the swelling ratio by setting the chemical potential to zero:

$$\frac{\partial}{\partial n_s}\left(\frac{\Delta G_{mix}}{k_b T}+\frac{\Delta G_{elastic}}{k_b T}\right)=0=[\ln(1-\upsilon_N)+(1-1/6)\upsilon_N+\chi\upsilon_N^2]+\left[\frac{\rho_p \tilde{V}_s}{M_c}(\upsilon_N^{1/3}-\upsilon_N/2)\right]$$

Eqn.(6)

ν_n is the volume fraction of polymer in the swollen gel and $1/\nu_n$ is the swelling ratio, χ is the Flory-Huggins interaction parameter, ρ_p is the polymer density and M_c is average molecular weight between cross-links and $\tilde{V}_s$ is the molar volume of the solvent. The factor (1-1/6) in the elastic term is a correction for small polymers, where the 6 is the number of monomer units for this calixarene (MC6AOAc). The ratio, $\frac{\rho_p}{M_c}$, corresponds to the crosslink density in the material. On the right side of this equation, the first set of square brackets corresponds to the mixing term of the derivative and the second set of brackets on the right corresponds to the elastic term of the derivative. Swelling always increases the elastic term and thus it is always positive. The mixing term in a swelling system is always negative. More swelling can be tolerated (larger $1/\nu_n$.) when χ is small (the mixing term is more negative allowing a larger elastic term). In addition, at constant χ, more swelling is tolerated when the cross-link density is lower and the $\tilde{V}_s$ is smaller.

In terms of our lithographic variables: exposure dose and developer solvent properties, exposure dose comes in to play through the ratio $\frac{\rho_p}{M_c}$, the polymer cross-link density. For a negative resist like calixarene higher doses means higher cross-link densities. The developer solvent properties come into play through the χ and $\tilde{V}_s$ parameters.

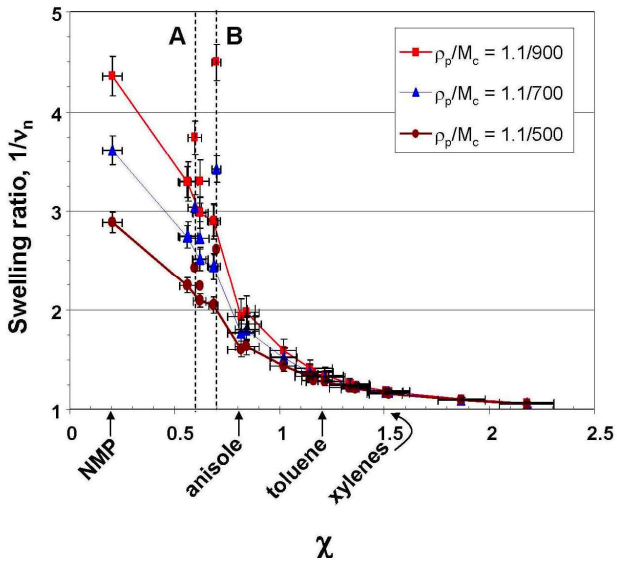

Figure 5. Plot of swelling ratio versus χ values for solvents interacting with calixarene. Three different values of cross-link density, ρ_p/M_c, are shown. The solid lines connecting data points are meant to guide the eye to solvents with larger molar volumes. The solvents used for development of the features shown in Fig. 4 are

noted at the bottom. Dotted lines A and B denote two solvents with smaller molar volumes. A is acetone with a molar volume of 74 cm^3/mole and B is acetonitrile with a molar volume of 52.6 cm^3/mole. At the same cross-link densities, these solvents will show considerably more swelling than the solvents with larger molar volumes.

Figure 5 shows a plot of the swelling ratio, $1/\nu_n$, versus χ. The solid lines are lines of constant dose (cross-link density) for solvents with larger molar volumes. The dotted lines (A and B) are lines of constant χ. The χ's for the solvents used in the contrast curves and developed features (Figs. 3 and 4) are noted on the bottom. The swelling ratio values were generated by numerically solving equation 6 for ν_n for a given χ, $\tilde{V}_s$ combination and for several values of $\frac{\rho_p}{M_c}$. The χ value's we used are from Table 2 and we used tabulated values for $\tilde{V}_s$.[10] Again, increasing values of $\frac{\rho_p}{M_c}$, the cross-link density, corresponds to increasing doses.

There are a couple of important features to point out in Figure 5, Firstly, the solid curves confirm that as the χ values increase, swelling decreases. Secondly, we look at the effects of molar volume, $\tilde{V}_s$. At constant χ, with decreasing $\tilde{V}_s$, swelling increases substantially. This is represented by the points on line A and B that lie above the solid

curves (solid lines are lines representing solids with $\tilde{V}_s$ over 90 cm^3/mol, the points above the curve at A and B are for solvents like acetone and acetonitrile with $\tilde{V}_s$ of 52 and 74 cm^3/mol respectively.). This is because of the effect of the elastic term in Eqn. 6. With a decrease in $\tilde{V}_s$, 1/ ν_n can increase without increasing the elastic contribution. And thus, at constant dose and constant χ, smaller $\tilde{V}_s$ means more swelling.

Finally, we look how dose (cross-link density) affects swelling. As discussed previously, lower dose (top, red curve) and lower χ allows more swelling of the cross-linked network. However, as the cross-linking density increases (bottom curve), lowering χ does not have as large an effect as at lower cross-linking densities (higher curve). The penalty to be paid, due to the elastic free energy term (Eqn. 6), with increasing cross-link density, reduces the effect of lowering χ. Thus changing the solvent (which changes χ) has less effect on swelling than at lower cross-link densities. In fact, in the limit of high cross-link density, the elastic term (Eqn. 6) will dominate such that no swelling will be tolerated, no matter what the χ value.

We can hence explain the effect of swelling on the contrast curves (Fig. 3). The gel dose, (on-set of a measurable feature thickness) increases with decreasing χ because the solvent wants to mix, swells the matrix, and solvates the uncross-linked material better than a larger χ solvent. Thus, for similar molar volumes, a smaller χ solvent should shift the negative contrast curve to the right as we see in the four solvents test in Fig. 3. The increasing contrast with decreasing χ (steeper slope, Fig. 3) is a consequence of the swelling being less dependent on χ as the cross-linking density increases. The difference in the swelling between the higher χ and lower χ materials decreases as the dose

increases and consequently the difference in thickness (Fig. 3 line B compared to line A). This implies a higher contrast for the low χ material and it is what we see in Fig. 3.

Furthermore we can explain the overall poorer line quality for lower χ materials over higher χ materials. (Fig. 4). Although resolved lines may be smaller, the damage due to swelling collapses the lines and causes the gel to stick together (see the NMP developed lines in Fig. 4). Calixarenes developed with xylenes, because of xylenes' higher χ, are not subject to the same extent of swelling, and show a better overall pattern quality (Fig. 4), even though the contrast is lower (Fig. 3). Yet, it is important to remember χ is still low enough to remove the unexposed, uncross-linked material (xylenes lie within the Hansen Solubility Sphere).

To summarize: generally materials with smaller χ values and similar molar volumes should give higher gel doses, higher contrast, and higher line resolution. However, if the swelling is profound enough, it will diminish line quality by causing lines to stick to neighboring features. Collapse during the drying process[16, 17] can also be exacerbated because the modulus of the material will also be affected by the swelling. The model to predict swelling described here is simple, makes all the assumptions inherent in the Flory-Huggins and Flory-Rehner theory, but still aids our understanding of contrast behavior in calixarene. It also suggests the ultimate resolution would be served not by choosing the lowest swelling solvent (largest χ or somewhere near the Hansen boundary), but by compromising with a moderately swelling solvent, moderate χ value, which has high contrast and better line resolution, but does not allow enough swelling to distort the pattern. The exact nature of where this compromise should be is the subject for future work.

Conclusions

We have measured the Hansen Solubility Sphere for Calixarene (MC6AOAc) by testing the solubility of the as-spun film with over 40 solvents and generating a three dimensional solubility map. The data was fit numerically to produce potential Hansen solubility sphere solutions. Sphere solutions were narrowed with additional considerations (Appendix 1). The difficulty in fitting the sphere arises because calixarene is a small molecule with a large sphere radius. Solid materials would have to be tested to more conclusively elucidate the sphere boundary and are beyond the scope of this work.

Nevertheless, narrowing the solutions, we were able to use the sphere to estimate the χ parameters for solvents interacting with calixarene. With this we used the Flory-Rehner equation and the thermodynamics of swelling to understand the contrast curves and pattern quality for several solvents developing e-beam exposed calixarene. Smaller χ values give higher contrast and the potential for higher resolution contrast but the choice of developers are limited due to the increased likelihood of swelling and feature collapse. Thus, the best pattern quality is obtained larger χ-value solvents. The optimum developer will have a χ value that offers a compromise between swelling and high contrast and is not necessarily the solvent which swells the material the least.

Acknowledgements

This work was supported by the Director, Office of Science, Office of Basic Energy Sciences, Materials Sciences and Engineering Division, of the U.S. Department of Energy under Contract No. DE-AC02-05CH11231.

Appendix 1. Discussion of the fitting of the Hansen sphere. Complications in narrowing the results.

The Hansen solubility sphere of calixarene was found by using the δ_d, δ_p, δ_h values from Table 1 to fit a sphere model that only included solvents, not non-solvents. To determine the initial starting values for the sphere-fitting algorithim, we calculated a median (*Mdn*) and standard deviation (*SD*) for each solubility parameter (i.e., δ_d, δ_p, δ_h) of all solvents in Table 1. In a three-dimensional space with $2\delta_d$, δ_p, and δ_h axes, the sphere center was estimated to reside in a volume extending from *Mdn – SD* to *Mdn + SD* of all three δ values for all solvents. We further estimated the sphere radius to have a range of values equal to the distance from the estimated sphere center to each individual solvent's position in the three-dimensional solubility space. Using the minimum, mean and maximum of the estimated ranges for δ_d, δ_p, δ_h, and radius, we generated 81 permutations to serve as the initial starting points for fitting the model. An algorithm based on the program presented by Gharagheizi[13] was employed to fit the solubility parameter values in Table 1 with each individual permutation-derived starting point. A simplex search method[18] was used for the sphere fitting, and each fitted solution was tested against the pre-specified model requiring the sphere to contain solvent, but not non-solvent substances. The code, written in MATLAB, is shown below:

```
soluble=load('delta_soluble_chemical')
insoluble=load('delta_insoluble_chemical')
insoluble(:,4)=zeros(length(insoluble(:,1)),1);
```

```
soluble(:,4)=ones(length(soluble(:,1)),1);
data=[soluble;insoluble];
[deltas,optsortdeltas,guesses]=HSP2(data,1e-3)



function [deltas,sort_opt_deltas, guesses]=HSP2(data, fit_tol)
delta_d=(data(:,1))';
delta_p=(data(:,2))';
delta_h=(data(:,3))';
solubility=(data(:,4))';


soluble_ind=find(data(:,4));
insoluble_ind=find(~data(:,4));
medians=median(data(soluble_ind,1:3));
stds=std(data(soluble_ind,1:3));
mins=medians-stds;
mins(find(mins<0))=0;
maxs=medians+stds;
average=mean([maxs;mins]);
average(4)=sqrt(sum(((maxs-mins)/2).^2.*[4 1 1]));
maxs(4)=max(sqrt(4*(medians(1)-delta_d(soluble_ind)).^2+(medians(2)-
delta_p(soluble_ind)).^2+(medians(3)-delta_h(soluble_ind)).^2));
mins(4)=min(sqrt(4*(medians(1)-delta_d(soluble_ind)).^2+(medians(2)-
delta_p(soluble_ind)).^2+(medians(3)-delta_h(soluble_ind)).^2));
start_pts=[maxs;average;mins]
output_abs=1;
option=optimset('TolFun', 1e-5);
guesses=zeros(1,4);
```

```
deltas=zeros(1,7);
cases=0;
for temp1=(start_pts(:,1))'
   guess(1)=temp1;
   for temp2=(start_pts(:,2))'
      guess(2)=temp2;
      for temp3=(start_pts(:,3))'
         guess(3)=temp3;
         for temp4=(start_pts(:,4))'
            guess(4)=temp4;
            cases=cases+1;
            disp(cases)
            guesses(cases,1:4)=guess;
            temp_guess=guess;
            res=1;
            trials=0;
            while res>fit_tol && trials<100
               trials=trials+1;
               [delta,res,exitflag,output]=fminsearch(@(xx) QF(xx, delta_d, delta_p,delta_h,solubility, output_abs), temp_guess, option);
               temp_guess=delta;
            end
            deltas(cases,1:4)=delta;
            deltas(cases,5)=res;
            deltas(cases,6)=exitflag;
            [deltas(cases,7),badfitdata]=chk_spherefit(delta, data, 0);
            if abs(deltas(cases,7))==res deltas(cases,7)=1;
            else deltas(cases,7)=0;
```

```
            end

            if length(badfitdata)==1
               if badfitdata==0
                  deltas(cases,8)=0;
               else
                  deltas(cases, 8)=length(badfitdata);
               end
            else
               deltas(cases, 8)=length(badfitdata);
            end

         end
      end
   end
end

  sort_opt_deltas=sortrows(deltas,5);
  function y=QF(x,delta_d,delta_p,delta_h,solubility, output_abs)
  d_d=x(1);
  d_p=x(2);
  d_h=x(3);
  R_o=x(4);
  R_a=sqrt(4*(d_d-delta_d).^2+(d_p-delta_p).^2+(d_h-delta_h).^2);
  for i=1:length(delta_d),
     if R_a(i)>R_o
        if solubility(i)==0
```

```
            A(i)=1;
        else
            A(i)=exp(R_o-R_a(i));
        end
    else
        if solubility(i)==0
            A(i)=exp(R_a(i)-R_o);
        else
            A(i)=1;
        end
    end
end

function [y,badfitdata]=chk_spherefit(x, data, output_abs)
d_d=x(1);
d_p=x(2);
d_h=x(3);
R_o=x(4);

delta_d=(data(:,1))';
delta_p=(data(:,2))';
delta_h=(data(:,3))';
solubility=(data(:,4))';
R_a=sqrt(4*(d_d-delta_d).^2+(d_p-delta_p).^2+(d_h-delta_h).^2);
badfitdata=0;
for i=1:length(delta_d),
    if R_a(i)>R_o
```

```
        if solubility(i)==0
            A(i)=1;
        else
            A(i)=exp(R_o-R_a(i));
            badfitdata=[badfitdata -i];
        end
    else
        if solubility(i)==0
            A(i)=exp(R_a(i)-R_o);
            badfitdata=[badfitdata i];
        else
            A(i)=1;
        end
    end
end
if length(badfitdata)>1    badfitdata=badfitdata(2:length(badfitdata)); end
%calculate the error function
if output_abs == 1
    y=abs(((prod(A))^(1/length(delta_d)))-1);
else
    y=(prod(A))^(1/length(delta_d))-1;
end
```

Fitting the solubility sphere to the data resulted in a large range of values for the solubility parameter for calixarene. This complication arises because calixarene is a low molecular weight material. The lower the molecular weight of the material, the larger the Hansen sphere radius. This can be understood by considering the thermodynamics of mixing. Within the ideal sphere boundary, the Gibb's free energy of mixing is negative

($\Delta G < 0$), outside $\Delta G > 0$, and at the boundary, $\Delta G = 0$. With smaller solutes, the entropic contribution is larger, allowing materials with much larger differences in solubility parameters to still be miscible. This is equivalent to a larger sphere radius.

To elucidate the boundary more clearly, we would have to investigate solvents with high δ_d, which implies solid solvent materials. Because it is difficult to test solid-solid mixing, we instead narrow the results using two methods. First we narrow it using the findings of Ho and Glinka.[19] Ho and Glinka showed that for a large number of organic solvents, there is correlation between the three Hansen components which limits the range of their values and allows one to be estimated if the other two are known. This correlation, summarized by the following two equations,

$$\beta + \gamma = 180° - 1.2883\alpha \qquad (7)$$

$$\beta - \gamma = \cos^{-1}\left(\frac{\cos^2\alpha}{\cos(1.2883\alpha)}\right) \qquad (8)$$

where $\cos\alpha = \delta_d/\delta_t$, $\cos\gamma = \delta_p/\delta_t$ and $\cos\beta = \delta_h/\delta_t$, was found to hold true for a random sampling of polymers. The worst correlation produces an error of 3 degrees for the equalities shown above. This left 40 solutions for the sphere fit.

Using equations 3 and 5, we calculated a χ value for each solvent studied with each of the remaining sphere fits. Each sphere fit will generate a different χ for each solvent because the center of the sphere, which corresponds to calixarenes solubility parameter is changes. We further narrowed the results by using the work of Flory. Flory showed that

polymer j and liquid i are completely miscible over the entire composition range if (page 378)[12]

$$\chi \leq 1/2[1+({}^{i}V/{}^{j}V)^{1/2}]^2 \qquad (9)$$

where V is the molar volume. These equations are strictly valid only if χ is independent of concentration. This is approximately true for "good" solvents. From equation 9, one can see that solvents with lower molar volumes will have smaller upper limits on χ's. We used this relation to eliminate sphere fits that did not give a χ which satisfied Eqn. 9 for acetone - the most limiting case of the solvents tested because of its small molar volume. This left 15 sphere fits which gave χ values which satisfied Eqn. 9 for acetone. We then calculated χ's for each solvent and each of the 15 sphere fits, giving 15 χ values per solvent. From these values, we found an average and standard deviation for each solvents χ value (Table 2). Using the average χ values, a relationship was found between the contrast and χ values for different developers (See text).

Table 1: Solvents used to tests solubility of calixarene. Hansen parameters from Ref. 6.

Solvent	δ_d	δ_p	δ_h	$\tilde{V}_s$	**Soluble?**
	$(MPa)^{1/2}$			cm^3/mole	
diethyl ether	14.5	2.9	5.1	104.8	N
methanol	15.1	12.3	22.3	40.6	N
t-butyl ether	15.3	3.4	3.3	90	Slightly
water	15.5	16.0	42.3	18.0	N
ethanol	15.8	8.8	19.4	58.5	N
2-butanol	15.8	5.7	14.5	92.0	N
isoamyl alcohol	15.8	5.2	13.3	109.4	Slightly
isopropyl alcohol	15.8	6.1	16.4	76.6	N
n-butanol	16	5.7	15.8	98.9	N
chloro acetaldehyde	16.2	16.1	9.0	60.4	N
propylene glycol	16.8	9.4	23.3	85.4	N
cyclohexane	16.8	0.0	0.2	108.7	Slightly
valeronitrile	15.3	11.0	4.8	103.8	Y
methyl isobutyl ketone	15.3	6.1	4.1	125.8	Y
acetonitrile	15.3	18.0	6.1	52.6	Y
acetone	15.5	10.4	7	74	Y
diethyl sulfate	15.7	14.7	7.1	131.5	Y
methacrylonitrile	15.8	15.1	5.4	83.9	Y
ethyl acetate	15.8	5.3	7.2	98.5	Y
diacetone alcohol	15.8	8.2	10.8	124.2	Y

amyl acetate	15.8	3.3	6.1	148.0	Y
hexyl acetate	15.8	2.9	5.9	165.0	Y
methyl ethyl ketone	16.0	9.0	5.1	90.1	Y
acetic anhydride	16.0	11.7	10.2	94.5	Y
ethyl lactate	16.0	7.6	12.5	115.0	Y
nitrioethane	16	15.5	4.5	71.5	Y
trans-crotononitrile	16.4	18.8	5.5	81.4	Y
tetrahydrofuran	16.8	5.7	8.0	81.7	Y
n,n-dimethyl acetamide	16.8	11.5	10.2	92.5	Y
xylenes	17.6	1.0	3.1	123.3	Y
anisole	17.8	4.1	6.7	119.1	Y
n-methyl-2-pyrrolidone	18.0	12.3	7.2	96.5	Y
toluene	18.0	1.4	2.0	106.8	Y
dichloromethane	18.2	6.3	6.1	63.9	Y
benzene	18.4	0.0	2.0	89.4	Y
benzyl alcohol	18.4	6.3	13.7	103.6	Y
chlorobenzene	19	8	4.1	102.1	Y
1,2 dichlorobenzene	19.2	6.3	3.3	101.4	Y

Table 2: Calculated χ_{12} for the interactions between solvents and calixarene.

Average of values calculated from 15 Hansen Sphere Fits.

Solvent	**Avg χ_{12}**	**Standard Deviation**
N-Methyl-2-Pyrrolidone	0.20	0.016
Acetonitrile	0.70	0.021
N,N-Dimethyl Acetamide	0.62	0.037
Tetrahydrofuran	0.62	0.044
Acetone	0.59	0.032
Methyl Ethyl Ketone	0.56	0.047
Methacrylonitrile	0.68	0.031
Trans-Crotononitrile	0.88	0.031
Anisole	0.81	0.065
Acetic Anhydride	0.84	0.038
Valeronitrile	0.84	0.057
Benzyl Alcohol	1.16	0.090
Benzene	1.23	0.076
Ethyl Acetate	1.02	0.062
Toluene	1.21	0.088
Diethyl Sulfate	1.14	0.039
Diacetone Alcohol	1.36	0.070
Xylenes	1.52	0.101
Ethyl Lactate	1.51	0.079
Methyl Isobutyl Ketone	1.33	0.097
Amyl Acetate	1.87	0.112

Hexyl Acetate	2.18	0.130

1. Geens, W.; Shaheen, S. E.; Wessling, B.; Brabec, C. J.; Poortmans, J.; Serdar Sariciftci, N. *Organic Electronics* **2002,** 3, (3-4), 105-110.
2. Yasin, S.; Hasko, D. G.; Carecenac, F. *J. Vac. Sci. Technol. B* **2001,** 19, (1), 311-313.
3. Cheng, J. Y.; Ross, C. A.; Smith, H. I.; Thomas, E. L. *Adv. Mater*. **2006,** 18, (19), 2505-2521.
4. Fujita, J.; Ohnishi, Y.; Ochiai, Y.; Matsui, S. *Appl. Phys. Lett.* **1996,** 68, (9), 1297-1299.
5. Fujita, J.; Ohnishi, Y.; Manako, S.; Ochiai, Y.; Nomura, E.; Matsui, S. *Microelectronic Engineering* **1998,** 41/42, 323-326.
6. Moreau, W. M., Development of Negative Resists. In *Semiconductor Lithography*, Plenum Press: New York, 1988; pp 506-514.
7. Prabhu, V.; Vogt, B. D.; Kang, S.; Rao, A.; Lin, E. K. *J. Vac. Sci. Technol. B* **2007,** 25, (6), 2517-2520.
8. Namaste, Y. M. N.; Malhotra, S.; Dems, B. C.; Rodrigues, F.; Obendorf, S. K. *Chem. Engin. Comm.* **1990,** 98, 47-54.
9. Novembre, A. E.; Masakowski, L. M.; Hartney, M. A. *Polym. Engin. Sci.* **1986,** 26, (16), 1158-1164.
10. Hansen, C. M., *Hansen Solubility Parameters: A User's Handbook*. CRC Press: Boca Raton, Florida, 1999.
11. Hildebrand, J. H.; Scott, R. L., *Solubility of Non-Electrolytes*. 3 ed.; Reinhold, New York, 1950.
12. Barton, A. F. M., *Handbook of Solubility Parameters and Other Cohesion Parameters*. 2nd ed.; CRC press: Boca Rotan, FL, 1991.
13. Gharagheizi, F. *J. Appl. Polym. Sci.* **2006,** 103, 31-36.
14. Flory, P. J. *J. Chem. Phys.* **1950,** 18.
15. Flory, P. J.; J. Rehner, J. *J. Chem. Phys.* **1943,** 11.
16. Tanaka, T.; Morigami, M.; Atoda, N. *Jpn. J. Appl. Phys. Part 1 - Regul. Pap. Short Notes Rev. Pap.* **1993,** 32, (12B), 6059-64.
17. Olynick, D. L.; Harteneck, B. D.; Veklerov, E.; Tendulkar, M.; Liddle, J. A.; Kilcoyne, A. L. D.; Tyliszczak, T. *J. Vac. Sci. Technol. B* **2004,** 22, (6), 3186-3190.
18. Lagarias, J. C.; Reeds, J. A.; Wright, M. H.; Wright, P. E. *SIAM J. Optimiz* **1998,** 9, (1).
19. Ho, D. L.; Glinka, C. J. *J. Polym. Sci. B* **2004,** 42, (23), 4337-4343.

Table of Contents Graphic

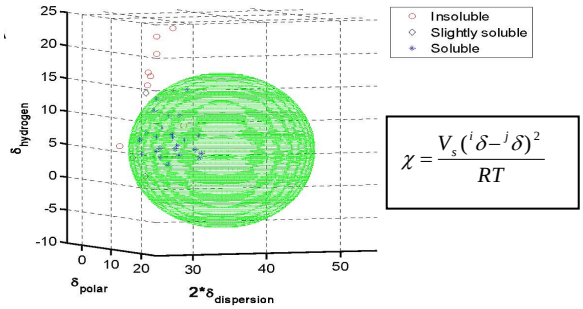

Hansen solubility sphere for calixarene (MC6AOAc)

The link between a negative high resolution resist contrast/developer performance and the Flory-Huggins parameter estimated from the Hansen solubility sphere.

Deirdre L. Olynick, Weilun L. Chao, Mark D. Lewis, Haoren Lu, Scott D. Dhuey, J. Alexander Liddle